EFFECTS OF THE SHAPE OF SURFACE MICROPORES ON THE PERFORMANCE OF A FACE SEAL

M. Mahbubur Razzaque* and M. Tanvir Rahman Faisal
Department of Mechanical Engineering
Bangladesh University of Engineering & Technology (BUET), Dhaka-1000, Bangladesh
Email: mmrazzaque@me.buet.ac.bd

Abstract: *A mathematical model is developed for the prediction of performance of a mechanical face seal with regular microstructure on its surface in the form of pores. Pores of right circular cylindrical, hemispherical and exponential profiles have been considered. A two dimensional steady state Reynolds equation is solved to get the hydrodynamic pressure distribution on an imaginary control area around a single pore. Consequently, the seal performance parameters such as seal clearance, friction torque and leakage across the seal are calculated. A parametric analysis is done for right circular cylindrical pores for a range of sealed pressure, pore size and pore ratio. Increase of pore ratio improves the seal performance up to a pore ratio of 12%, beyond which no improvement of the seal performance is possible. The optimum pore size depends on the sealed pressure as well as on the pore profile. Through a comparison of the performance of face seals with different pore profiles hemispherical pores are recommended for enhancement of performance. For any pore profile, the seal performance improves with the increase of pore depth as long as the depth is less than 1.5 times of the pore radius.*

Keywords: *Face seal, seal performance, surface micropore, pore profile, pore ratio.*

INTRODUCTION

Mechanical face seals are widely used in pumps, compressors, turbo-machineries and powered vessels for sealing rotating shafts operating under conditions of high fluid pressures and high speeds. Non-contacting-type face seals are most popular as they provide lower leakage, less maintenance and longer life. However, when face seals fail, they do so completely. The most probable cause of non-contacting seal failure is the occurrence of intermittent contacts between the seal faces. Therefore, contact elimination as well as decreasing leakage flow is of prime importance in non-contacting face seals, especially in critical applications where seal failure may have severe consequence. It has been shown[1-4] that the texture of the sliding surfaces of a face seal affects its performance. Recent advances in micro-fabrication techniques have broadened the scope of improvement of face seal performance using deliberately machined surface textures on the seal faces.

Hamilton et al.[4] conducted some wonderful experiments on the effects of micro-asperities on load support and leakage of face seals. Anno et al. proposed the so-called small tilt theory[5] in an attempt to explain the experimental results of Hamilton et al. and subsequently[6] studied the performances of both micro-asperities and micro-pores using their theory. Lai[7] showed that even micro-pores of small depth are able to generate load through hydrodynamic action. Etsion and Burstein[8] developed a model to study the performance of a face seal with hemispherical micro-pores arranged in a rectangular array on the seal surface. In a following paper, Etsion et al.[9] presented experimental results with laser textured seal faces to show the enhancement of a face seal's life.

Nomenclature

A	Total annular seal area [m^2]	r_i	Seal inner radius [m]
B_r	Seal balance ratio [-]	r_o	Seal outer radius [m]
F	Friction force [N]	R	Nondimensional pore radial coordinate [-]
F_c	Closing force [N]	R_o	Pore radius [m]
h	Local film thickness [m]	R_1	Half - length of a control cell [m]
h_{av}	Average seal clearance [m]	S	Pore ratio [-]
h_o	Nominal seal clearance [m]	T	Friction torque [N-m]
h_p	Pore depth [m]	U	Average circumferential velocity [m/s]
H	Nondimensional local film thickness [-]	W	Opening force [N]
p_f	Spring pressure [MPa]	x, z	Pore Cartesian coordinate [m]
p_s	Hydrostatic pressure [MPa]	X, Z	Nondimensional coordinates [-]
p	Hydrodynamic pressure [MPa]		
P	Nondimensional hydrodynamic pr. (p/Λ) [-]		**Greek symbols**
P_t	Total nondimensional pressure [-]	Ψ	h_p/h_o
Q	Leakage [m^3/s]	ξ	R_1/R_o
r	Pore radial coordinate [m]	Λ	Bearing number

Recently, Faisal[10] and Faisal and Razzaque[11] developed a mathematical model for face seals with micro-pores of arbitrary shape. Based on this model, they[12] have presented a parametric study on the performance of face seals with exponential pores. Better performance could be achieved with proper selection of pore size and pore ratio. The preferable percentage of pore ratio was found to be 15% as the improvement of performance slows down at higher values of pore ratio. The optimum pore diameter was close to 10 μm for exponential pores.

This paper reports the result of a study on the performance of face seals with surface micro-pores of right circular cylindrical, hemispherical and exponential profiles. The seal performance parameters such as seal clearance, friction torque and leakage across the seal are calculated for right circular cylindrical pores for a range of sealed pressure, pore size and pore ratio. The present results are compared with the previously published results with the other two profiles.

PHYSICAL MODEL

Consider, identical micro-pores are evenly distributed over the surface area of an annular mechanical face seal following a rectangular grid as shown in Fig. 1(a). Along the plane of the seal surface, the pores are circular and each pore has a radius of R_o. In the plane perpendicular to the seal surface, the pores may have different cross sections. In the present work, rectangular (for right circular cylindrical pores), half circular (for hemispherical pores) and exponential (for exponential pores) cross-sections, each with a maximum pore depth of h_p at the center, have been considered. The detail of the pore geometries is shown in Fig. 1(b). The distance between two neighboring pores, $2R_1$, is large enough so that the interaction among the pores is negligible. Each pore is located at the center of an imaginary "control cell" of size $2R_1 \times 2R_1$, as shown in figure 1(c). The mating surface of the seal is smooth and parallel and moving with uniform circumferential velocity, U. The two surfaces are separated by a nominal film thickness h_o. The clearance gap is filled by a Newtonian fluid with viscosity, μ. The hydrodynamic pressure distribution over each control cell is exactly the same and the hydrostatic pressure drops linearly from the outer boundary to the inner boundary of the seal.

MATHEMATICAL MODEL

The hydrodynamic pressure over a single control cell in the clearance gap is given by the Reynolds equation:

$$\frac{\partial}{\partial x}\left(h^3\frac{\partial p}{\partial x}\right)+\frac{\partial}{\partial z}\left(h^3\frac{\partial p}{\partial z}\right)=6\mu U\frac{\partial h}{\partial x} \qquad (1)$$

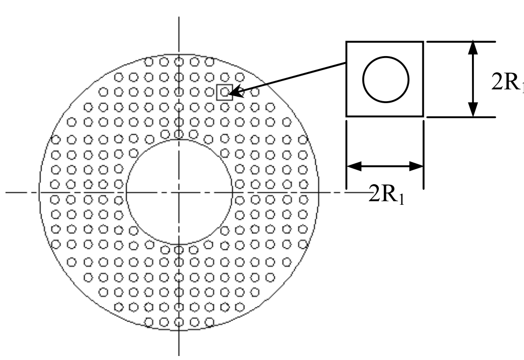

Figure 1(a): Pore distribution on the sliding surface of a mechanical face seal.

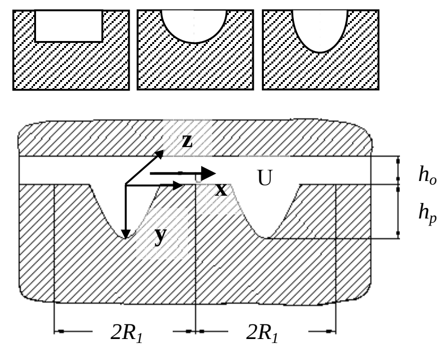

Figure 1(b): *Top:* cross section of the pores - rectangular (left), half circular (middle) and exponential (right). *Bottom:* Pore geometry.

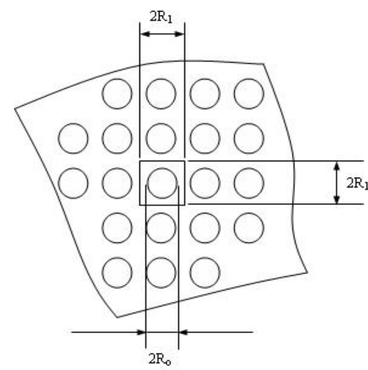

Figure 1(c): Control cell with coordinate system.

Here, h is the local film thickness and is a function of the geometry of the pores. Outside the pore, where $x^2 + z^2 \geq R_o$ in the region $2R_1 \times 2R_1$ of a control cell, the local film thickness, h is simply equal to the nominal film thickness, h_o. Over the pores, the local film thickness, $h = h_o + h'$, where, $h' = h_p$ at the center of the pore; i.e. at r = 0. For the remaining area of the pore, where, $x^2 + z^2 < R_o$, the local film thickness and hence h′ depends on the profile of the pore in the x-y plane. The expressions of h′ for different pore geometries are listed below.

For rectangular profile: $h' = h_p$

For half circular profile: $h' = h_p\sqrt{1-x^2} = R_o\sqrt{1-r^2}$

For exponential profile:

$$h' = h_p \exp\left(\frac{r}{R_o}\ln\frac{h_o}{h_o+h_p}\right) + h_o\left[\exp\left(\frac{r}{R_o}\ln\frac{h_o}{h_o+h_p}\right)-1\right]$$

In addition to the appropriate expressions for local film thickness, the solution of Eq.(1) requires the boundary conditions: p = 0 at $x = \pm R_1$ and $z = \pm R_1$. Using the relations

$$X=\frac{x}{R_o},\ Z=\frac{z}{R_o},\ H=\frac{h}{h_o},\ \xi=\frac{R_1}{R_o},\ R=\frac{r}{R_o},\ \psi=\frac{h_p}{h_o},\ P=\frac{p}{\Lambda}$$

and $\Lambda = \frac{6U\mu R_0}{h_0^2}$, the nondimensional form of Eq.(1) may be obtained as:

$$\frac{\partial}{\partial X}\left(H^3\frac{\partial P}{\partial X}\right)+\frac{\partial}{\partial Z}\left(H^3\frac{\partial P}{\partial Z}\right)=\frac{\partial H}{\partial X} \qquad (2)$$

Here, outside the pore boundary, i. e. for $X^2 + Z^2 \geq 1$, the nondimensional local film thickness, H = 1 and the expressions for H over the pore, where $X^2 + Z^2 < 1$, are listed below for the three profiles under consideration.

For rectangular profile: $H = 1+\Psi$

For half circular profile: $H = 1 + \psi\sqrt{1 - R^2}$

For exponential profile: $H = (1+\psi)\exp[-R\ln(1+\psi)]$

The nondimensional boundary conditions are: P = 0 at both $X = \pm\xi$ and $Z = \pm\xi$. If the pore ratio is S; that is if the pore area covers S fraction of the seal area, then for a single control cell of size $2R_1 \times 2R_1$, it may be shown that,

$$\xi = \frac{1}{2}\left(\frac{\pi}{S}\right)^{0.5} \tag{3}$$

SOLUTION PROCEDURE AND CALCULATION

Equation (2) and the boundary conditions have been discretized using finite difference scheme to get a system of linear equations. The hydrodynamic pressure at various grid points of a control cell is obtained by solving the system of equations by successive over relaxation (SOR) method. Total nondimensional local pressure at each control cell is $P_t = P + P_s$. Here, the nondimensional local hydrostatic pressure P_s is estimated by the following equation based on the assumption that the hydrostatic pressure drops linearly from the seal outer to inner boundary.

$$p_s = p_i + (p_o - p_i)\frac{r - r_i}{r_o - r_i} \tag{4}$$

where, $P_s = \Lambda p_s$; p_i and p_o are the hydrostatic pressures at the seal inner and outer radii, respectively.

The pores closer to the seal inner radius are prone to cavitation. The hydrostatic pressure P_s over such a pore is not high enough to eliminate cavitation. According to the half-Sommerfeld condition, the hydrodynamic pressure P is made zero at each point of a cavitating control cell where negative total pressure is encountered. At a given value of Ψ i.e. a given nominal film thickness, the calculation proceeds along a radial line from the inner radius r_i, towards the outer radius r_o. The average hydrodynamic load per unit area of the n-th control cell can then be calculated from

$$\overline{W_n} = \int_{-\xi}^{\xi}\int_{-\xi}^{\xi} P dX dZ \tag{5}$$

Equation (5) is evaluated numerically using Simpson's 1/3rd rule and the dimensional load support over the n-th cell is given by, $W_n = \overline{W_n}\,\Lambda R_o^2$. The total opening force tending to separate the seal ring is,

$$W = \pi(r_o^2 - r_i^2)(p_o - p_i) + \sum_{n=1}^{N_s} W_n$$

For different values of Ψ which depends on the seal clearance h_o, the hydrodynamic load per unit area, $\overline{Wn}$ and hence the total opening force, W may be calculated in the same way. But the seal clearance is actually not known a priory. The equilibrium seal clearance is the established by a balance between the seal opening force W and the seal closing force F_c given by

$$F_c = \pi(r_o^2 - r_i^2)[p_f + B_r(p_o - p_i)]$$

Here, p_f is the pressure exerted by the spring to close the seal clearance. B_r is balance ratio, which is usually less than unity for a highly pressurized seal. To find the seal clearance, a certain clearance is assumed and the corresponding opening force W is calculated and compared with the closing force F_c. The entire procedure is repeated with a different value of seal clearance until the balance is achieved. Neglecting the effect of pressure gradient, the total friction over the annular sealing area, A can be written as,

$$F = \int_{\text{nonpore area}} \mu \frac{U}{h} dA + \int_{\text{pore area}} \mu \frac{U}{h} dA$$

The first integral can be written in terms of pore ratio, S as,

$$F = \pi\mu\frac{U}{h_o}(1 - S)(r_o^2 - r_i^2)$$

which is same for all three profiles under consideration. The evaluation of the second integral depends on the choice of the profile of the pores. For rectangular profile of the right circular cylindrical pores, the second integral becomes,

$$F = \pi\mu\frac{U}{(1+\psi)h_o} S(r_o^2 - r_i^2)$$

Similar results for hemispherical pore are given in Etsion and Burstein[8] and for exponential pore in Razzaque and Faisal[12]. Therefore, those will not be repeated here and in the rest of this paper the performance of the seal with right circular cylindrical pore will be presented and compared with the performance of the seals with hemispherical and exponential pores. Now the friction force for the seal with right circular cylindrical pore can be obtained from the above three equations as

$$F = \pi\mu\frac{U}{h_0}(r_0^2 - r_i^2)\left[1 - S\frac{\psi}{(1+\psi)}\right] \tag{6}$$

By defining nondimensional friction force as

$$\overline{F} = \frac{F.h_p}{\pi\mu U(r_0^2 - r_i^2)}$$

Eq. (6) may be written in nondimensional form as

$$\overline{F} = \psi - S\frac{\psi^2}{1+\psi} \tag{7}$$

Thus, the friction torque of the seal is $T = Fr_m$, where, $r_m = (r_o + r_i)/2$. Based on Poiseuille's law, the dimensional leakage across the seal is given by

$$Q = \frac{\pi h_o^3 r_m}{6\mu}\frac{p_o - p_i}{r_o - r_i} \tag{8}$$

For calculation, it is assumed that the annular seal has inner and outer radii, respectively of 28.4 mm and 31.1 mm. The spring for closing the seal exerts a pressure, p_f = 0.415 MPa and the balance ratio, B_r is set to 0.8. Since the width of the seal is small, the radial variation of the sliding velocity may be neglected and the mean sliding velocity U is taken to be 9.5 m/s. The viscosity of the sealing fluid, μ is 25 mPa-s. The sealed pressure is varied from 0.5 MPa to 3.0 MPa. The iterative procedure to balance the opening force to the closing force is stopped when the seal clearance falls below certain limiting value, which is set to 0.01μm in the present calculation.

RESULTS AND DISCUSSION

The performance parameters such as seal clearance, friction torque and leakage are calculated as a function of pore diameter for right circular cylindrical, hemispherical and exponential pore profiles at four pore ratios such as 2.5%, 11.25%, 15% and 20%. Since the results for hemispherical and exponential profiles are already published[8, 12], this paper will report typical results for only the right circular cylindrical profile. The results will be compared with the results for hemispherical and exponential profiles to investigate the effects of the shape or geometry of the pores on the face seal performance.

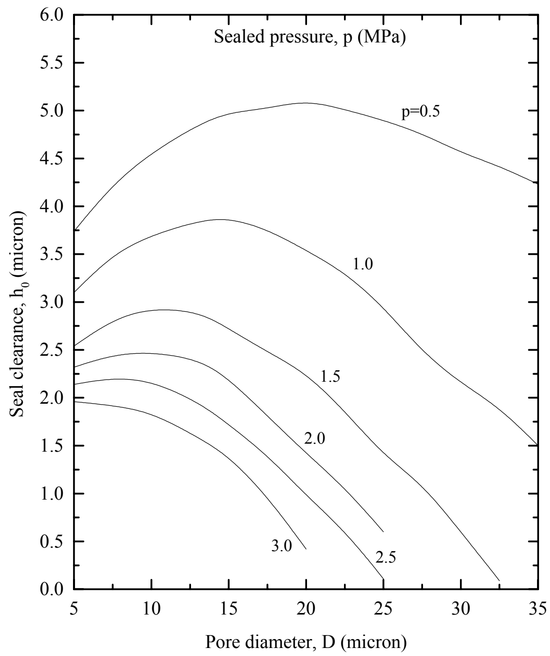

(a): Pore ratio of 11.25 %

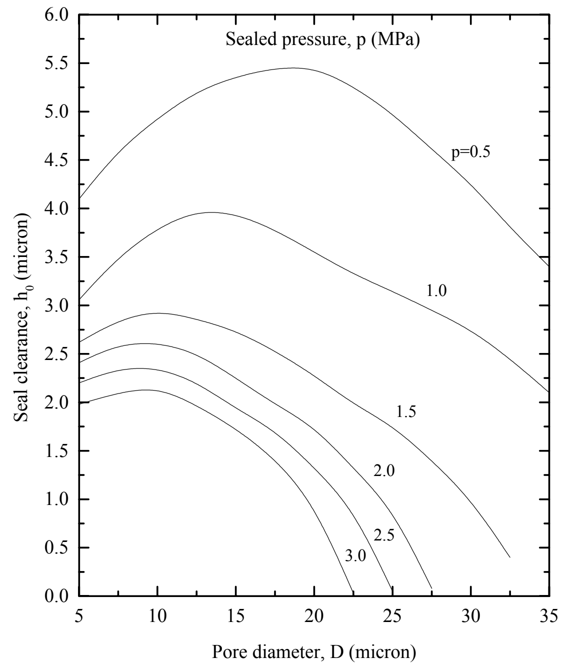

(b): Pore ratio 15 %

Figure 2: Seal clearance vs. pore diameter at different sealed pressures for rectangular pore.

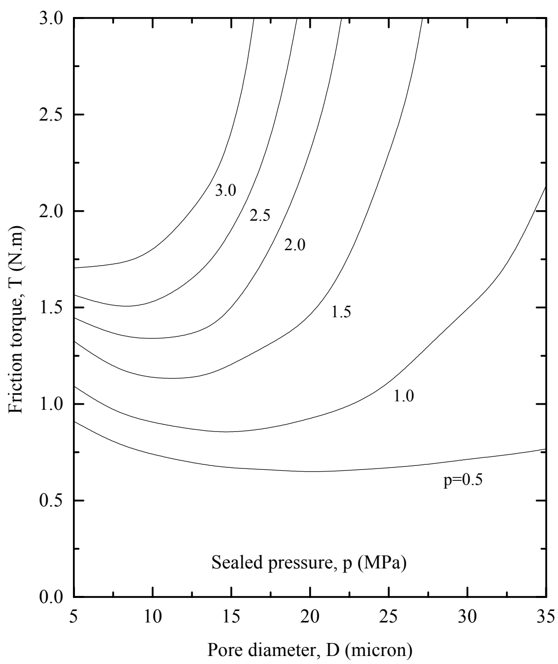

(a): Pore ratio of 11.25 %

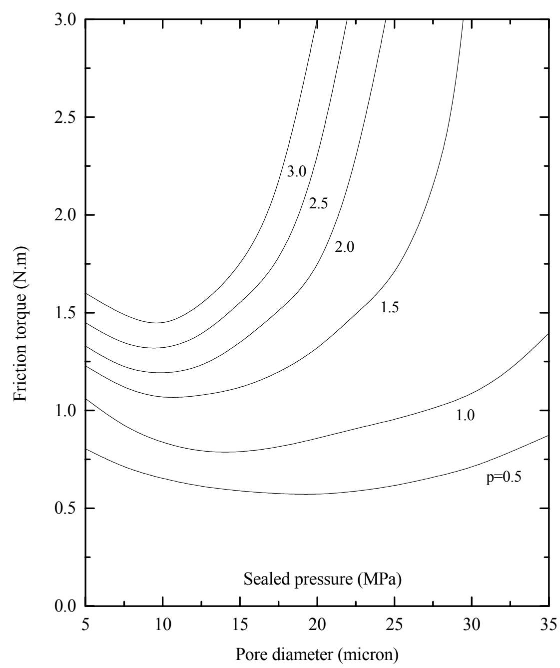

(b): Pore ratio 15 %

Figure 3: Friction torque vs. pore diameter at different sealed pressures for rectangular pore.

Figures 2(a) and 2(b) show the effect of pore size on seal clearance for right circular cylindrical pore profile with two pore ratios, when the sealed pressure varies from 0.5 to 3 MPa. Pore size is given as the diameter of the pore, R_o, in the sliding plane and the pore ratio is defined as the ratio of the area covered by the pores to the total seal area expressed in percentage. It is evident from the figure that at a small sealed pressure, there exists an optimum pore size for which the seal clearance is the maximum. For example, as shown in figure 2(a) for a pore ratio of 11.25% and a sealed pressure of 0.5 MPa, the optimum pore diameter is about 20 µm. At this size the seal clearance is the

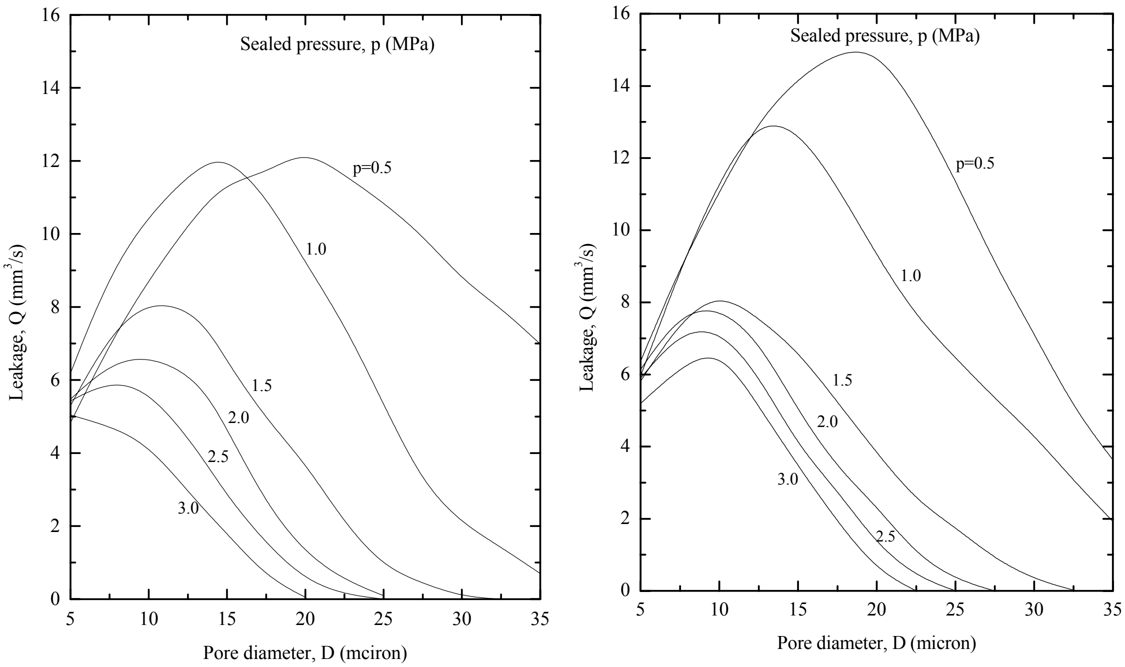

(a): Pore ratio of 11.25 % **(b):** Pore ratio 15 %

Figure 4: Leakage vs. pore diameter at different sealed pressures for rectangular pore.

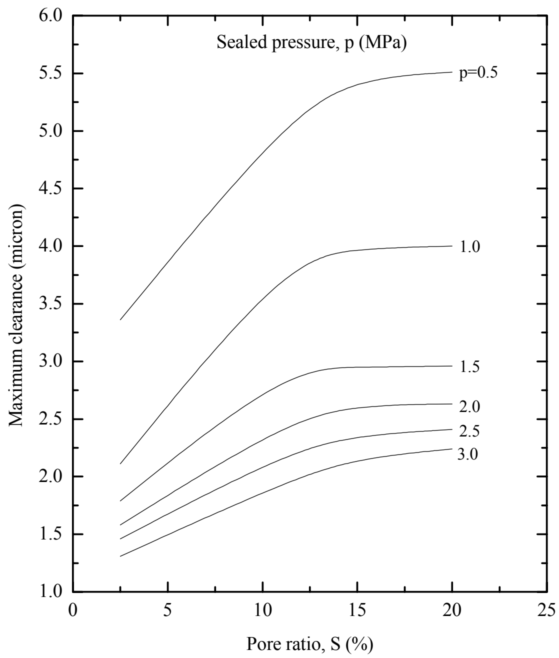

Figure 5: Maximum seal clearance vs. pore ratio at different sealed pressures for rectangular pore.

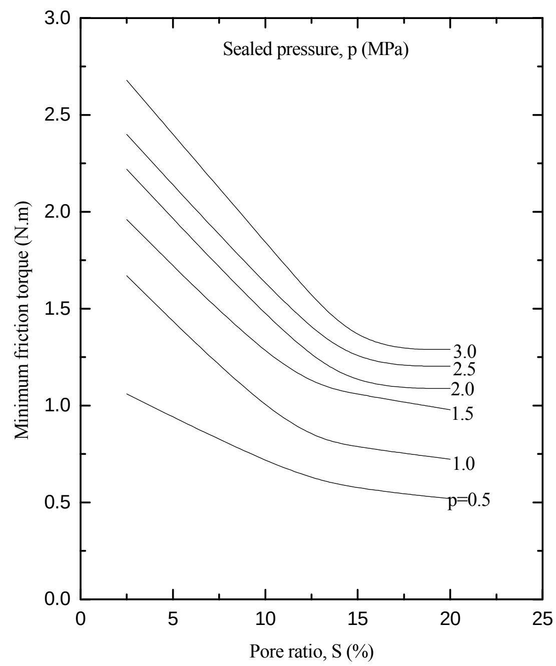

Figure 6: Minimum friction torque vs. pore ratio at different sealed pressures for rectangular pore.

maximum and is about 5 µm. This is the point of operation where opening force tends to balance the closing force and hence the axial stiffness becomes the maximum. Beyond this point, the seal clearance decreases rapidly. As the sealed pressure increases, the seal clearance decreases. The size of the pore diameter where the maximum seal clearance occurs reduces with sealed pressure. But as the pore ratio increases, the seal clearance and hence the maximum seal clearance also increases. In Fig. 2(b) similar behavior of seal clearance with respect to pore diameter is observed for the pore ratio of 15%. For sealed pressure of 0.5 MPa at this pore ratio, the optimum seal clearance is 5.4 µm. The pore size for this optimum value is 20 µm.

Figures 3(a) and 3(b) show the relationship between friction torque and pore diameter for right circular cylindrical pore profile with two pore ratios, when the

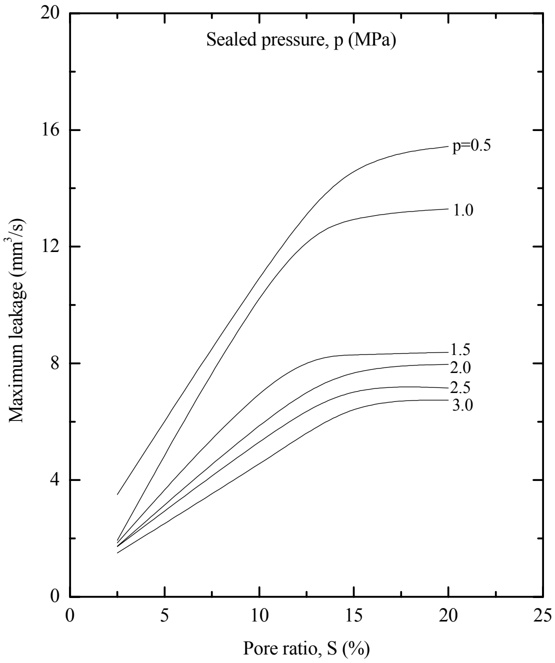

Figure 7: Maximum leakage vs. pore ratio at different sealed pressures for rectangular pore.

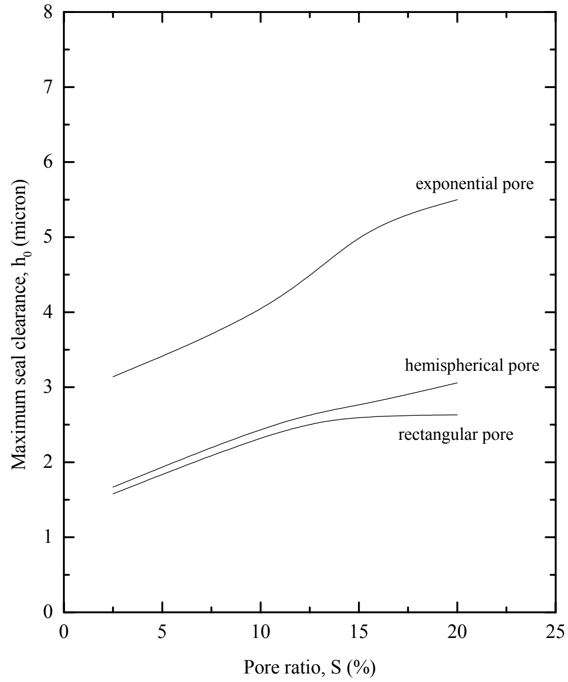

Figure 8: Maximum seal clearance vs. pore ratio among different pore geometries at sealed pressure of 2.0 MPa.

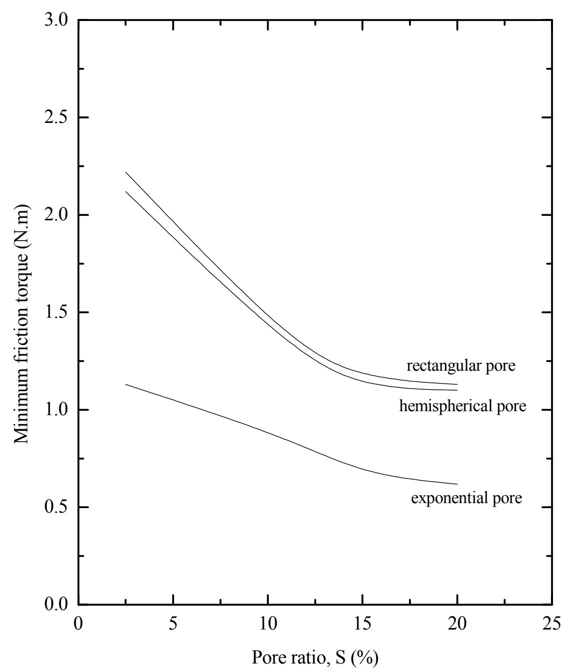

Figure 9: Minimum friction torque vs. pore ratio among different pore geometries at sealed pressure of 2.0 MPa.

sealed pressure varies from 0.5 to 3 MPa. It is seen that for both 11.25% and 15% pore ratios, the friction torque exhibits minimum value at the point of maximum clearance. At a given sealed pressure, the magnitude of the friction torque remains almost the same for all pore diameters below the optimum pore diameter. Beyond the optimum pore diameter the friction torque increases significantly. It is interesting to note that at large pressures, the influence of the pore diameter on the friction torque is more crucial. At small pressures, the effect of pore diameter is relatively less important. It may be noticed that at any sealed pressure, the friction torque is less at the higher pore ratio. Moreover, at higher pore ratio, the effect of the sealed pressure on the friction torque is less pronounced, which is very desirable for an application where variation in the sealed pressure is likely to be encountered.

Figures 4(a) and 4(b) show the relationship of leakage with pore diameter at different sealed pressures. Maximum leakage is observed at the point of maximum seal clearance. Beyond the critical pore diameter the leakage drops sharply. The magnitude of leakage increases by a considerable amount with the increase of pore ratio which actually indicates the importance of leakage when higher pore ratios are considered.

Figures 5 to 7 show the relationships of maximum seal clearance, minimum friction torque and maximum leakage with pore ratios for right circular cylindrical pore profile. It is clearly visible that the seal clearance and the leakage increase whereas the friction torque decreases with the increase of pore ratio. The improvement of seal performance with the increasing percentage of pores continues up to a pore ratio of 12%. However, the rate of improvement of seal performance declines as the pore ratio is increased beyond 12%. This is because with the increase of the area of pores on the sealing surface the effects of cavitation become more prominent and consequently the hydrodynamic load increases and the friction torque decreases at a faster rate. Moreover, the possibilities of interaction among the pores increases and the assumption of negligible interaction among the pores becomes invalid.

Figures 8 and 9, give the comparative results for the three pore geometries investigated. Figure 8 compares the effect of pore profiles on the behavior of the maximum seal clearance with respect to pore ratio at a sealed pressure of 2.0 MPa, whereas Fig. 9 compares the effect of pore profiles on the behavior of friction torque under the same operating condition. After a close inspection of the results,

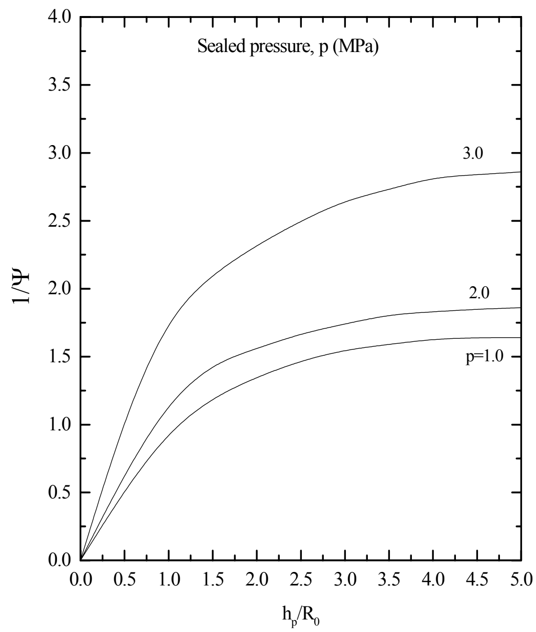

Figure 10: $1/\Psi$ vs. h_p/R_o at different sealed pressures for exponential pore with 20% pore ratio.

it may be concluded that for the three profiles, the optimum pore ratio lies between 12% and 15% and the qualitative trend of the seal performance is similar. However, quantitatively the exponential pores give the higher seal clearance, which will cause higher leakage. So as a compromise between the seal clearance and the leakage and considering the fabrication complexities, the hemispherical pores will be the best choice.

The average seal clearance for different pore profiles may be estimated as follows:

For rectangular pore: $h_{av} = h_o(1 + S\psi)$

For hemispherical pore: $h_{av} = h_0\left\{1 + S\psi\sqrt{1 - R^2}\right\}$

For exponential pore:

$h_{av} = h_o\{1 - S + (1+\psi)S\ \exp[-R\ln(1+\psi)]\}$

In the above calculations, the ratio of pore depth to nominal film thickness, Ψ was taken to be unity. For a given Ψ, the average seal clearance for rectangular and hemispherical pores exhibit almost same numerical results. But the exponential pore yields a higher value of h_{av} than the other two. That is why friction torque is the lowest for exponential pores and close to each other for rectangular and hemispherical pores.

Figures 10 depicts the effect of pore depth on seal clearance, where the maximum seal clearance at different sealed pressures is plotted against pore depth. The pore depth is nondimensionalized by pore radius. The maximum seal clearance is nondimensionalized by pore depth and turned into $1/\Psi$. It is observed that the seal clearance increases with the increase of pore depth. The increment rate of seal clearance diminishes after a pore depth ratio of 1.5 for both rectangular and exponential pores. It implies that it is not possible to enhance seal performance by making pore depth larger than 1.5 times of the pore radius.

CONCLUSION

A mathematical model has been presented to study the performance of a mechanical face seal with right circular cylindrical micropores on the surface. A parametric analysis shows that better performance in terms of higher clearance and smaller friction torque can be achieved with proper selection of pore size and pore ratio. The preferable percentage of pore ratio is 12 as performance improvement becomes negligible at higher values of pore ratio. The optimum pore diameter depends on sealed pressure and pore ratio. A comparison of the performance of face seals with different pore profiles reveals that the hemispherical pore is the best choice for enhancement of performance. It is observed that the seal clearance increases with the increase of pore depth. However, it is not possible to enhance seal performance by making pore depth larger than 1.5 times of the pore radius.

REFERENCES

1. Salama, M. E., 1952, “The Effect of Macroroughness on the Performance of Parallel Thrust Bearings”, Proc. I MechE., Vol. 163, pp. 149-158,
2. Pape, J. G.. 1968, “Fundamental Research on Radial Face Seals.” ASLE Trans., Vol. 11, No. 4, pp. 302-309.
3. Etsion, I., 1980, “The Effect of Combined Coning and Waviness on the Separating Force in Mechanical Face Seals”, Journal of Mech. Engg. Sci., Vol. 22, No. 2, pp. 59-64.
4. Hamilton, D. B., Walowit, J. A. and Allen, C. M., 1966, “A Theory of Lubrication by Microirregularities”, Journal of Basic Engineering, Trans. ASME, Vol. 88, No. 1, pp. 177-185.
5. Anno, J. N., Walowit, J. A. and Allen, C. M., 1968, “Microasperity Lubrication.”, Journal of Lubrication Technology, Trans. ASME, Vol. 91, No. 2, pp. 351-355.
6. Anno, J. N., Walowit, J. A. and Allen, C. M., 1969, “Load Support and Leakage from Microasperty Lubrication of Face Seals”, Journal of Lubrication Technology, Trans. ASME, Vol. 9, No. 4, pp. 726-731.
7. Lai, T. W., 1980, “Development of Non-contacting, Non-leaking Spiral Groove Liquid Face Seals”, J. Lubrication Engineering, Vol. 50, No. 8, pp. 625-640.
8. Etsion, I. and Burstein, L., 1996, “Model of Mechanical Seals with Regular Micro Surface Structure”, STLE Tribology Transactions, Vol. 39, No. 3, pp. 677-683.
9. Etsion, I., Kligerman, Y. and Halperin, G., 1999, “Analytical and Experimental Investigation of Laser-Textured Mechanical Seal Faces“, STLE Tribology Transactions, Vol. 42, No. 3, pp. 511-516.
10. Faisal, M. T. R., 2006, “Effect of Pore Geometry on Face Seal Performance”, Masters thesis, Dept. of Mechanical Engineering, Bangladesh University of Engineering and Technology (BUET), Dhaka-1000, Bangladesh.
11. Faisal, M. T. R. and Razzaque, M. M., 2006, “The Effects of Pore Ratio on the Performance of Mechanical Face Seals having Microirregularities in the Form of Exponential Pores”, Proc. 3rd Int. Conf. on the Technological Advances of Thin Films and Surface Coatings - THINFILMS 2006, Singapore, pp. 304-305.
12. M. M. Razzaque and M. T. R. Faisal, 2007, "Performance of Mechanical Face Seals with Surface Micropores", J. Mechanical Engineering, IEB, vol.37, pp 77-80.

.